ZANCO Journal of Pure and Applied Sciences
The official scientific journal of Salahaddin University-Erbil
https://zancojournals.su.edu.krd/index.php/JPAS

ISSN (print):2218-0230**, ISSN (online):** 2412-3986**, DOI: http://dx.doi.org/10.21271/zjpas**

RESEARCH PAPER

Applying the SWMM Software Model for the High Potential Flood-Risk Zone for Limited Catchments in Erbil City Governorate

Bakhtiyar A. Ali[1], Dana K. Mawlood[2]

[1]Department of Water Resources Engineering, College of Engineering, Salahaddin University-Erbil, Kurdistan Region, Iraq
[2]Department of Civil Engineering, College of Engineering, University of Salahaddin, Erbil, Kurdistan Region, Iraq

A B S T R A C T:
Every year, the vicinity of the Council of Ministers is frequently inundated. Due to the area's shifting land use and the inadequacy of the existing drainage system to handle the rising drainage loads, KRG decided to build two box sewers (BS). The drainage system in the study area will be evaluated, and the effectiveness of the BS construction in reducing flood amounts in the study area, as well as comparing the capacity of the drainage system before and after the BS construction using EPA SWMM version 5.2. The data used in this study are rain data and drainage network dimensions. Since the rain gauge station at the research area did not directly provide the 2-hour time series rainfall data, it was created using the Alternating Block Method (ABM) by determining a rainfall hyetograph from 5-year, 25-year, and 100-year Intensity-Duration-Frequency (IDF) curves. Following the specification and inputs of all EPA SWMM 5.2 parameters, six simulation scenarios were run based on the before and after adding (BS). Prior to the addition of (BS), the number of flooded nodes for the first three scenarios was (33, 31 and 28), and it was reduced to (25, 22 and 19) nodes. According to the findings, the drainage planning design for the study area is not adequate to handle the drainage load of the area, either now or in the future.

KEY WORDS: Box Sewer SWMM; IDF Curve; Alternating Block Method;
DOI: http://dx.doi.org/10.21271/ZJPAS.35.4.05
ZJPAS (2023) , 35(4);41-50 .

1.INTRODUCTION:

Urban flooding is one of the most serious issues facing modern society. Every year, flash floods occur in Erbil City as a result of an intense rainfall event. Stormwater flooding is a concern that is less likely to occur in well-planned cities than in uncontrolled ones. Rapid yet haphazard urbanization, which increases the amount of impervious surface, exacerbates urban flooding (Huong and Pathirana, 2013).

The society has suffered significant losses in terms of both lives and property as a result. Waterlogging and flooding are major concerns for such unplanned and unprepared towns, causing property damage and disrupting residents' daily lives due to high intensity and frequency climate and weather events such as excessive rainfall in short periods of time (Patz et al., 2005). Urban flooding is typically increased by unplanned urban growth and development because it obstructs the natural flow of water (Booth, 1991, Douglas et al., 2008).

Since Erbil is an unplanned city, good storm water outlet planning should take these concerns into account. In this situation, it is urgently necessary to upgrade and improve the drainage system design in order to prevent the

* **Corresponding Author:**
Bakhtiyar Ahmed Ali
E-mail: bakhtiyar.ali@su.edu.krd or baxtiyar2010@gmail.com
Article History:
Received: 17/10/2022
Accepted: 28/12/2022
Published: 30/08 /2023

failure of the sewage system, transportation infrastructure, manholes, etc. Due to high rains in 2021, especially in October and December, flash flooding situations are common in various areas of Erbil City, causing significant financial loss, and severe commercial, trade, and employment opportunity losses. Due to these problems, the community is more aware of the need for flood risk management and land use planning policies to protect them from urban flooding.

Urban flooding is caused by a variety of factors, including the invasion of water bodies and canals, solid waste clogging pipes and conduits, and low storm water carrying capacity. Urban flooding causes extensive infrastructural damage, as well as loss of life, loss of property, and the spread of infectious diseases. In order to forecast flash flood conditions, comprehensive storm network analysis and flood management are needed in urban areas. As a result, the Kurdistan Regional Government took many actions in response to the floods, including building multiple ponds and small dams in the northeast of Erbil. Most of the natural canals and streams that brought water from the high elevations outside of Erbil city into the city their paths were blocked and they needed to be cleaned and expanded, which was one of the reasons of floods.

To further safeguard the research area and the city's center, some roadway culverts have been widened. The KRG, in particular the Ministry of Municipalities, decided to build two box sewers (BS), which are 1200 meters long and size (2 * 2 m), starting in front of the Council of Ministers to a 60-meter street near the silo because it is the location of the confluence of other neighborhood sewerage networks. The study area's sewage system was unable to handle the amount of runoff that occurred during heavy rains in a short amount of time.

In this study, the drainage network of the study area will be evaluated, and the effectiveness of the BS construction in reducing flood amounts in the study area and the capacity of the drainage network before and after the construction of the box drainage network. SWMM is a rainfall-runoff model that is used to simulate the quantity and quality of surface runoff from urban areas, (Rossman, 2015).

(Agarwal and Kumar, 2020) investigated a study that utilized the SWMM model to simulate the urban flood in Vijayawada. For the 2 year and 1-year return periods, the IDF curve created for those periods displays maximum intensities of 156.49 mm/hr, and 98.14 mm/hr, respectively, with an interval of 5 min. The findings demonstrate that the time to peak and runoff peak are greater in places with dense population and impervious surface, and that the length of conduits and roughness coefficient are the main parameters influencing peak flow in the study. The model's performance in simulating runoff and peak runoff in the urban catchment is demonstrated by the results.

(Alisawi, 2020) examined the study to assess the effectiveness of a proposed sewer line (SSL) by utilizing a pipe jacking technology in order to boost the sewage capacity and decrease sewer floods in the historic pilgrimage city of Karbala, Iraq (PJS). The storm water management model SWMM 5.0 was used for this. Sewage discharge during the busiest pilgrimage season reaches 200% of the capacity of the present sewer line, according to simulations of the existing sewer system. It is possible to reduce the water depth in a sewer pipe by 78% by installing a 2.5 m diameter SLL by PJS at a depth of 12 to 22 m. The decrease in water depth at the sewer pipe can reduce sewer overflow by up to 70% if the system is constructed and maintained properly. The methods in the paper can be applied, with the necessary modifications, in any area with a similar problem.

(Mohammad et al., 2021) conducting a study using the Storm Water Management Model (SWMM) to simulate the storm sewer network in the study area under the 9.6 mm/hour design rainfall intensity. The intensity tripled, increasing the risk of flooding by 43%. The suggested approach lowers the percentage of flooding to 31% by adding new pipes to connect the collateral lines in the Al-Andalus and Al-hoz suburbs. The results of the network simulation were compared before and after the new lines were introduced. The results indicated the network's gain from the suggested solution. While just 70 of the 225 total manholes in Ramadi's central business district's new storm sewage system remain wet after further pipe lines are added, there are a total of 96 flooded manholes in the system.

2. MATERIALS AND METHODS

2.1. Model Setup

The research area's sub-catchment discretization in SWMM is carried out using a map of different drainage outlets and routes from Google Earth Pro. By separating it into 23 sub-catchments, the area is represented schematically in Fig. 1. The runoff from these sub-catchments is collected in 100 nodes that are linked by various linkages and discharge at two outlets. Every sub-catchment parameter, such as the invert level, depth, slope, area, and percentage of imperviousness, is set in the model. To define the percentage slope for each sub-catchment, a slope map created from DEM data of the study area with 30 m resolution is shown in Fig. 2a. The Alternating Block Method used to calculate a 2-hour rainfall hyetograph for return periods of 5, 25, and 100 years is utilized as input data to run the model. The Horton Method is employed in the model to calculate infiltration, and the Dynamic Wave Method is taken into consideration for flow routing.

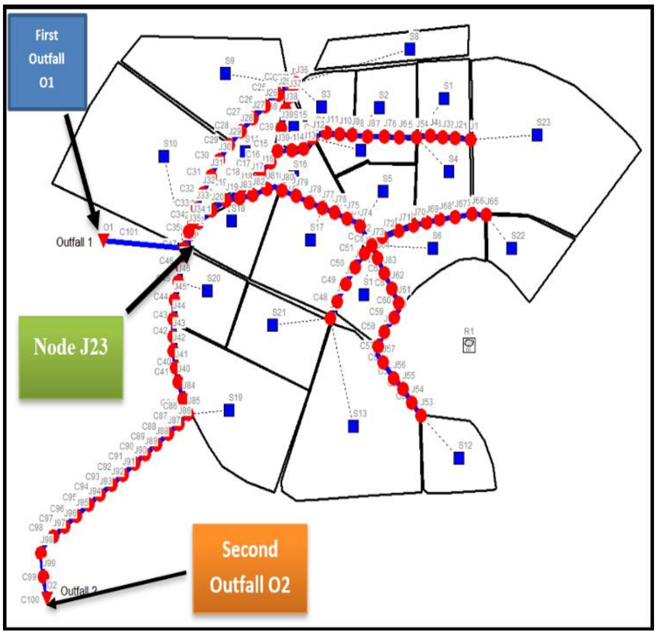

Figure 1: Discretization of Study Area

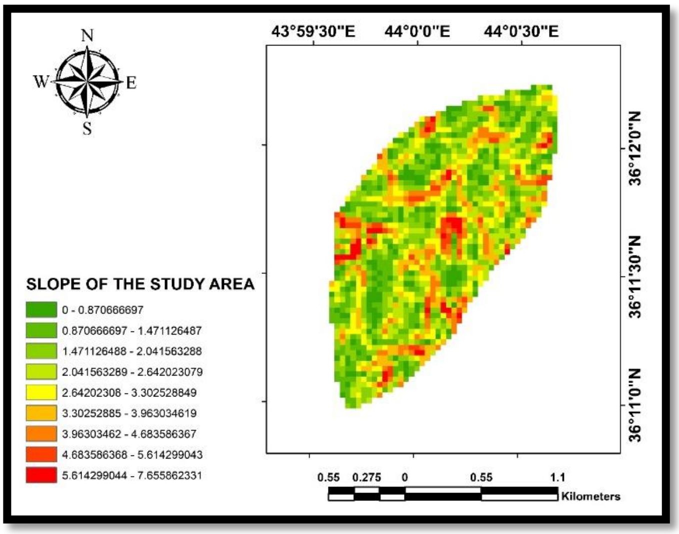

Figure 2a: Slope Map of the Study Area

2.2 Study Area

Erbil is the capital of the Kurdistan Region and is located in a flat, hilly region. The research area is a low area relative to the surroundings and is situated in the city center between (36° 11' 12.63" N, 43° 59' 46.51" E) and (36° 12' 11.45" N, 44° 0' 57.83" E). The research area is a populated area that experiences annual flooding from short-duration, high-intensity rainfalls. The study area begins in the Tairawa neighborhood in the northeast and ends in front of the Council of Ministers in the southwest. A satellite image of the study area is shown in Fig. 2b.

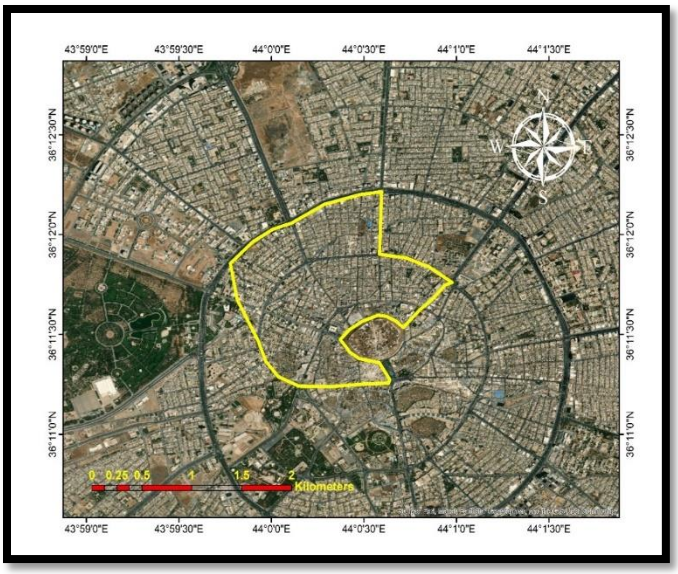

Figure 2b: Study Area

2.3 Data Collection

The study area's drainage system is quite old, and its design cannot endure intense rains because there are a lot of runoffs and the area is primarily impervious. The Erbil Water and Sewerage Directorate supplied the data for this study. The sewerage system comprises three 2*2 m-sized concrete box sewerage networks, and there is also a fourth one that includes two concrete box sewers (2*2 m) to pass the flow through and reduce flood damage that is under construction and partially completed. Additionally, there are two circular concrete drains that deliver water to the front of the Council of Ministers with diameters of 1.0 and 1.25 meters.

2.4 Climate Data

The semiarid climate of Erbil has low summertime humidity and moderate wintertime humidity. In the summer, there are often days with temperatures above 45 °C, and in the winter, it is frequently chilly and damp, with lows of 0 °C. More than 400 mm of rain falls annually on average over the long term. The rainy season normally starts in the middle of October and lasts until the end of May. December and January are the coldest months, while July and August are the hottest months.

2.5 Gumbel Distribution

Utilizing the rainfall data obtained from Erbil Meteorological Station for the period from 1992 to 2022, Intensity Duration Frequency IDF curves are generated following the procedures explained below.
The theory of extremes was first presented by Gumbel (1958) by considering the distribution of the highest or lowest values found in repeated samples. The Gumbel hypothesis is the distribution that is most frequently used for IDF analysis since it is appropriate for modelling maximum data. It is rather simple and only appropriate for extreme events (peak data or peak rainfalls). The following equation can be used to determine the intended rainfall depth for a specific time period (Chow et al., 1988)

$$XT = x^{-} + Kt.Sx \quad \text{.......................... Eq 1}$$

The maximum daily rainfall for the past 31 years was filtered and hourly precipitation data have been calculated using IMD empirical equation:

$$Pt = P24\left(\frac{T}{1440}\right)^{\frac{1}{3}} \text{.......................... Eq 2}$$

Where:
Pt= the precipitation depth required for a duration less than 24 hrs in mm
$P24$ = the daily rainfall depth in mm
T = the duration time in minutes

For the hourly precipitation values, mean and standard deviations have been calculated:

$$x^{-} = \frac{1}{n}\sum_{i=n}^{n} pi \quad \text{..........................Eq 3}$$

$$Sx = \sqrt{\left[\frac{1}{n-1}\sum_{i=1}^{n} (Pi - Pav)^2\right]} \text{ .... Eq 4}$$

Where:
x^{-} and Sx the mean and standard deviation of different specified rainfall durations respectively
Frequency factors ($\boldsymbol{Kt}$) shall be calculated from the formula:

$$kt = -\frac{\sqrt{6}}{\pi}\ln\left(\ln\frac{Tr}{Tr-1}\right) \text{ .... Eq 5}$$

Where:
Tr is return period in years.
The value of kt and maximum 2-hour Rainfall for different return period shown in Table.1.

Table (1) 2-Hour Maximum Rainfall Depth for Different Return Periods.

Return Period (year)	Kt	Maximum Rainfall depth (mm)
5	1.1695	29.88
25	2.49388	40.719
100	3.5867	49.662

2.6 Rainfall Hyetograph by Using Alternating Block Method

One of the most important input parameters for the SWMM program is the rainfall hyetograph. In this study, the author conducted the synthetic rainfall hyetographs for 2 hours of rainfall with a 10-minute interval for return periods of 5 years, 25 years, and 100 years for Erbil Meteorological Rain Gauge Station data from 1992–2022, shown in Fig. 3, Fig. 4, and Table 2. One straightforward method for creating a design storm from an IDF curve is the alternate block method. The design storm generated by this method describes the depth of rainfall that will occur for a total duration of (Td = n t) in (n) consecutive time intervals of duration (t). The rainfall intensity is extrapolated from the IDF curve for each of the durations based on the design return period (Butler and Davies, 2011). This hyetograph shows a distinct return period for rain and a duration of rain that is equal to or less than Td. Additionally, the center portion of the main hyetograph with a rainfall duration of Td will be used when the rainfall duration is less than Td (Behbahani, 2009).

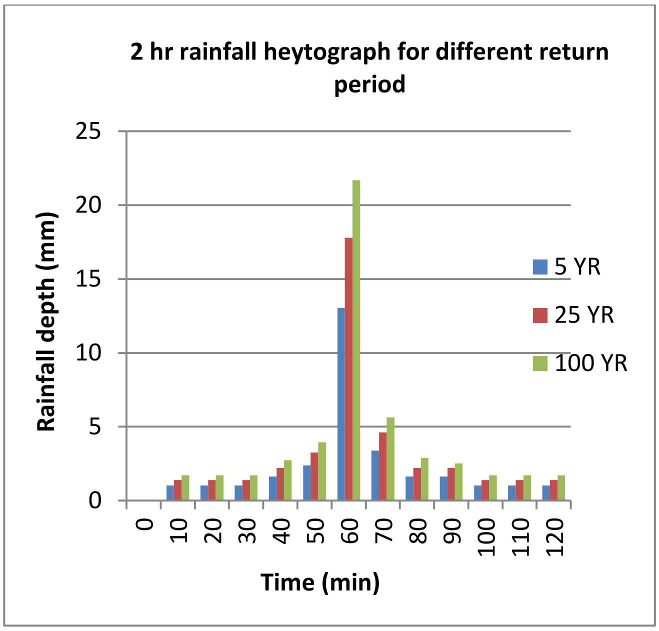

Figure 3: Rainfall Hyetograph

Table (2) Rainfall Depth and Intensity with 10 minutes interval.

Time interval (Min)	5-year rainfall depth (mm)	Rainfall Intensity (mm/hr)	25-year rainfall depth (mm)	Rainfall Intensity (mm/hr)	100-year rainfall depth (mm)	Rainfall Intensity (mm/hr)
0	0.000	0.0	0.0	0.0	0.0	0.0
10	1.027	78.311	1.400	106.711	1.707	130.145
20	1.027	49.333	1.400	67.224	1.707	81.987
30	1.027	37.650	1.400	51.304	1.707	62.571
40	1.631	30.684	2.222	41.811	2.726	51.273
50	2.381	26.504	3.244	36.115	3.957	44.290
60	13.052	23.718	17.785	32.320	21.691	39.418
70	3.392	21.210	4.623	28.903	5.638	35.250
80	1.631	19.329	2.222	26.340	2.897	32.124
90	1.631	17.886	2.224	24.347	2.510	29.692
100	1.027	16.696	1.400	22.752	1.707	27.747
110	1.027	15.738	1.400	21.447	1.707	26.156
120	1.027	14.94	1.400	20.360	1.707	24.831
Sum	29.88		40.72		49.662	

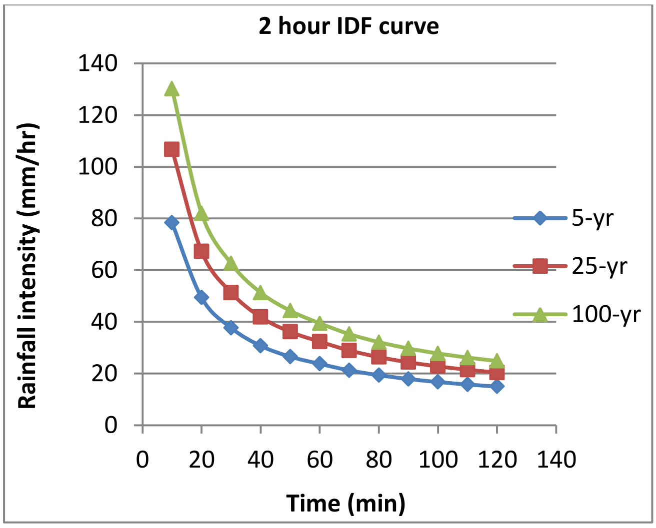

Figure 4: 2-Hour IDF Curve

3. RESULTS AND DISCUSSION

SWMM was used to simulate the peak runoff, node water depth, water elevation profile, outlet inflow, and sewer design. The chosen area is separated into 23 sub-catchments, and each junction node is planned with appropriate sewer lines and an effective slope. After determining the intensity duration frequency (IDF) curves for each return period, it is observed that the SWMM has generated the peak runoff for a 2-hour rainfall depth for the three different return periods of 5 years, 25 years, and 100 years. The 2-hour rainfall hyetograph is determined by using the alternating block method as an input parameter for various return periods. After completing the simulation, compare the model's output before and after adding the extra box sewer.

3.1. Outfall Loading

The findings demonstrated that the addition of box sewer had a positive impact on flood water transportation and reduction, as well as reducing the load on the first outlets. Prior to the addition of the additional network, the first outlet was unable to pass the full volume of accumulated water. The outfall loading and maximum flow rate for the three return periods are shown in Table 3, both before and after additional box sewer construction.

Table 3: Outfall Loading

Outfall loading	**Flow Frequency %**	**Average Flow %**	**Maximum Flow CMS**	**Total Volume 10^6 ltr**	**Outfall loading**	**Flow Frequency %**	**Average Flow %**	**Maximum Flow CMS**	**Total Volume 10^6 ltr**
		Before adding box sewer					**After adding box sewer**		
		100-yr					**100-yr**		
O1	99.19	2.269	18.915	54.538	**O1**	99.2	1.403	12.043	33.74
					O2	95.7	0.927	7.796	22.086
		25-yr					**25-yr**		
O1	99.14	1.968	17.058	47.027	**O1**	99.14	1.159	10.624	28.939
					O2	95.47	0.771	6.654	18.716
		5-yr					**5-yr**		
O1	99.36	1.548	14.057	36.838	**O1**	99.04	0.859	8.495	22.556
					O2	95.06	0.55	5.114	14.33

3.2. Node Flooding

The number of flooding nodes was (33, 31 and 28) for the three different return periods of 100, 25 and 5 years prior to the construction of the box sewer. It has since decreased to (25, 22 and 19) nodes, meaning that even though the number of flooding nodes has decreased, there are still a significant number of nodes that are flooded. According to rainfall data, more rain is possible in two hours, causing more flooding. Table 4, compares the number of flooding nodes for each return period before and after adding the box sewer.

Table (4) Flooding Node for Various Return Periods Before and After adding Box Sewer

Node	**Max. Flood Rate CMS**	**Node**	**Max. Flood Rate CMS**	**Node**	**Max. Flood Rate CMS**	**Node**	**Max. Flood Rate CMS**	**Node**	**Max. Flood Rate CMS**	**Node**	**Max. Flood Rate CMS**
	Before 100-yr		**After 100-yr**		**Before 25-yr**		**After 25-yr**		**Before 5-yr**		**After 5-yr**
J81	0.02	**J81**	0.015	**J81**	0.0016	**J81**	0.001	**J49**	0.0032		
J71	0.0523	**J71**	0.0456	**J49**	0.0068	**J49**	0.0057	**J50**	0.0056		
J51	0.048	**J51**	0.0412	**J50**	0.0884	**J50**	0.0602	**J67**	0.0044		
J50	0.120	**J50**	0.10	**J51**	0.0358	**J51**	0.0348	**J51**	0.03	**J51**	0.0029
J49	0.008	**J49**	0.006	**J45**	0.0268			**J81**	0.0009		
J45	0.044			**J67**	0.0272	**J67**	0.0194	**J64**	0.0132		
J42	0.100			**J64**	0.0316	**J64**	0.0272	**J42**	0.054		
J69	0.0268	**J69**	0.0144	**J44**	0.0832			**J43**	0.0456		
J64	0.036	**J64**	0.0188	**J42**	0.0928			**J71**	0.06	**J71**	0.060
J63	0.0784	**J63**	0.07	**J43**	0.0960			**J76**	0.1404	**J76**	0.137
J44	0.1052			**J71**	0.0336	**J71**	0.0256	**J40**	0.0772		
J41	0.1084			**J41**	0.1084			**J70**	0.1584	**J70**	0.1278

J43	0.1456			**J63**	0.0528	**J63**	0.050	**J65**	0.1284	**J65**	0.1272
J66	0.148			**J62**	0.1328	**J62**	0.1204	**J68**	0.0872	**J68**	0.081
J79	0.1572	**J79**	0.1551	**J78**	0.1556			**J41**	0.1036		
J65	0.1748	**J65**	0.1712	**J65**	0.1608	**J65**	0.1588	**J66**	0.1052	**J66**	0.100
J70	0.2108	**J70**	0.2088	**J68**	0.1772	**J68**	0.1505	**J82**	0.146	**J82**	0.1396
J78	0.2332	**J78**	0.2295	**J46**	0.1824			**J79**	0.1056	**J79**	0.0964
J67	0.234	**J67**	0.2288	**J76**	0.1896	**J76**	0.1876	**J69**	0.1944	**J69**	0.1887
J68	0.2492	**J68**	0.2403	**J70**	0.1968	**J70**	0.1875	**J80**	0.2008	**J80**	0.200
J82	0.2636	**J82**	0.2616	**J79**	0.1272	**J79**	0.1033	**J74**	0.2164	**J74**	0.2130
J76	0.27	**J76**	0.2687	**J73**	0.2344			**J78**	0.2184	**J78**	0.2152
J74	0.2836	**J74**	0.216	**J82**	0.2436	**J82**	0.2336	**J72**	0.2236	**J72**	0.2216
J62	0.306	**J62**	0.290	**J75**	0.2752	**J75**	0.2608	**J52**	0.2472	**J52**	0.2424
J46	0.3372			**J80**	0.2980	**J80**	0.280	**J77**	0.2692	**J77**	0.2648
J75	0.3484	**J75**	0.3477	**J83**	0.3164	**J83**	0.298	**J67**	0.0978	**J67**	0.089
J80	0.3728	**J80**	0.370	**J40**	0.3372			**J75**	0.3268	**J75**	0.3004
J40	0.5936			**J52**	0.4452	**J52**	0.4264	**J48**	0.424	**J48**	0.404
J72	0.6508	**J72**	0.6492	**J72**	0.4656	**J72**	0.4492				
J52	0.6528	**J52**	0.652	**J77**	0.5464	**J77**	0.536				
J77	0.7628	**J77**	0.76	**J48**	0.723	**J48**	0.686				
J83	0.784	**J83**	0.772								
J48	0.954	**J48**	0.901								

3.3. Total Inflow for Node J23 and Outfall O1 After Adding Box Sewer:

The total inflow per node J23 and first outfall O1 reduces significantly for two main reasons after the model has run for all three return periods. First of all, all the water that was previously flowed to the first outfall O1 is now much of the water goes to the second outfall O2 after the building of the new box sewers. The second reason is that nodes J40 to J47 used to discharge all inflow to node J23, but after the addition of box sewer it became part of the network, they no longer discharge water to node J23, but instead send it to the box sewers. Before adding box sewers, the maximum inflow of node J23 for different return periods was (18.4, 13.1, and 12.07) CMS, which is now reduced to (16.96, 13.81, and 11.3) CMS for all three return periods. When the total inflow of the first outfall O1 is compared, it is clear that the addition of the box sewer had a significant impact, as it decreased from (17.56, 14.95, and 11.61) CMS to (11, 9.16, and 7.53) CMS for the three return periods. This means that the construction of the box sewer reduced the total inflow of node J23 and the first outfall O1. Figure 5 and 6 shows the total inflow differences for the three return periods for node J23 and outfall O1 and compares them with each other.

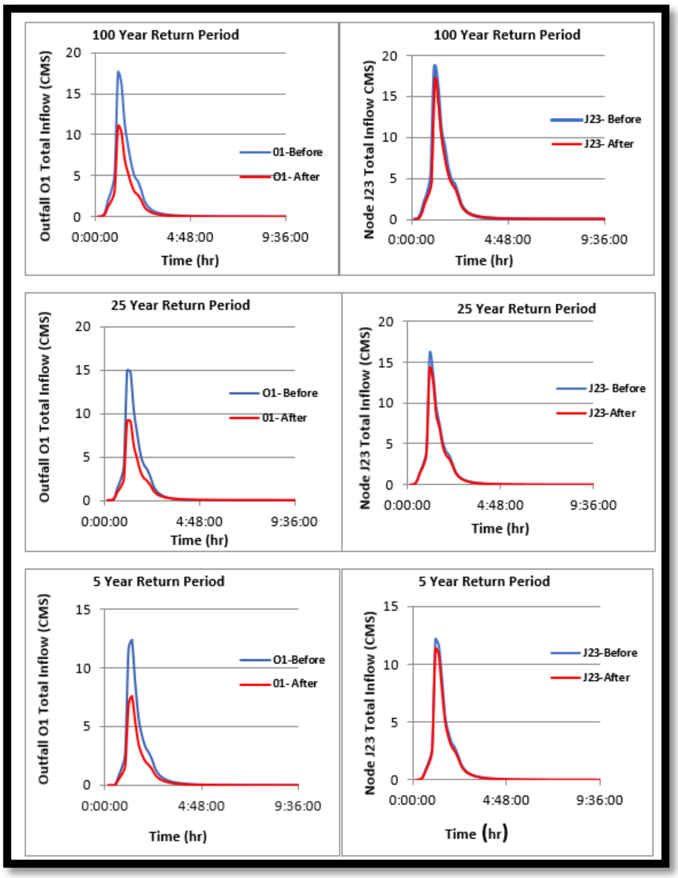

Figure 5-6: Total Inflow of Outfall 1 and J23 for Different Return Periods

3.4. Depth of Nodes for Various Return Periods:

For three distinct return periods, before and after the addition of the box drainage networks, Table 5 displays the maximum depth of the nodes. Because the node and conduit section in some manholes is unable to pass all runoff water, flooding has developed in the region, and the water level has reached ground level or higher. Using this knowledge, it is possible to identify the precise lowered node levels required to create the appropriate slope and flow in various conduit networks. Although adding the box drainage network was somewhat effective in reducing the amount of flooding and node depths, this does not solve the problem of flooding occurring in the study area. It is necessary that the entire drainage system in the study area be redesigned, and the sections should be enlarged.

Table (5): Node maximum depth for various return periods

Node	Max. depth 100-yr	Max. depth 25-yr	Max. depth 5-yr	Node	Max. depth 100-yr	Max. depth 25-yr	Max. depth 5-yr
Before				**After**			
J1	1.17	0.97	0.73	**J1**	1.16	0.97	0.73
J2	1.12	0.91	0.66	**J2**	1.12	0.91	0.66
J3	1.22	0.99	0.72	**J3**	1.22	0.99	0.72
J4	1.36	1.13	0.85	**J4**	1.36	1.13	0.85
J5	1.36	1.14	0.86	**J5**	1.36	1.14	0.86
J6	1.4	1.17	0.88	**J6**	1.4	1.17	0.88
J7	1.46	1.23	0.94	**J7**	1.46	1.23	0.94
J8	1.38	1.15	0.87	**J8**	1.38	1.15	0.87
J9	1.41	1.18	0.9	**J9**	1.41	1.18	0.9
J10	1.38	1.16	0.88	**J10**	1.38	1.16	0.88
J11	1.33	1.11	0.83	**J11**	1.33	1.11	0.83
J12	1.41	1.17	0.87	**J12**	1.41	1.17	0.87
J13	1.5	1.23	0.92	**J13**	1.5	1.23	0.92
J14	1.48	1.19	0.86	**J14**	1.49	1.19	0.86
J15	1.92	1.51	1.15	**J15**	1.94	1.52	1.15
J16	2	1.56	1.19	**J16**	2.0	1.56	1.19
J17	2	1.60	1.22	**J17**	1.99	1.59	1.22
J18	2.09	1.79	1.44	**J18**	2.09	1.78	1.45
J19	2.2	2.04	1.72	**J19**	2.18	2.03	1.72
J20	2.08	1.96	1.75	**J20**	2.07	1.95	1.74
J21	1.93	1.83	1.64	**J21**	1.91	1.82	1.62
J22	1.72	1.64	1.45	**J22**	1.72	1.63	1.45
J23	1.27	1.18	1.03	**J23**	0.92	0.84	0.72
J24	0.64	0.55	0.42	**J24**	0.64	0.55	0.42
J25	0.63	0.53	0.41	**J25**	0.63	0.53	0.41
J26	0.6	0.51	0.39	**J26**	0.6	0.51	0.39
J27	0.64	0.54	0.42	**J27**	0.64	0.54	0.42
J28	0.63	0.53	0.41	**J28**	0.63	0.53	0.41
J29	0.6	0.51	0.39	**J29**	0.6	0.51	0.39
J30	0.64	0.54	0.42	**J30**	0.63	0.54	0.41
J31	0.64	0.54	0.41	**J31**	0.62	0.52	0.41
J32	0.63	0.52	0.39	**J32**	0.58	0.49	0.37
J33	0.71	0.61	0.43	**J33**	0.57	0.48	0.36
J34	0.94	0.84	0.67	**J34**	0.65	0.55	0.4
J35	1.17	1.07	0.92	**J35**	0.85	0.76	0.62
J36	1.47	1.11	0.74	**J36**	1.47	1.11	0.74
J37	1.56	1.22	0.84	**J37**	1.56	1.21	0.84

J38	1.66	1.3	0.93	**J38**	1.66	1.3	0.93
J39	1.75	1.42	1.03	**J39**	1.74	1.4	1.03
J39-1	1.84	1.49	1.12	**J39-1**	1.82	1.49	1.12
J48	1.5	1.5	1.5	**J48**	1.5	1.5	1.5
J49	1.5	1.5	1.5	**J49**	1.5	1.5	1.5
J50	1.5	1.5	1.5	**J50**	1.5	1.5	1.5
J51	1.5	1.5	1.5	**J51**	1.5	1.5	1.5
J52	1.5	1.5	1.5	**J52**	1.5	1.5	1.5
J53	0.61	0.53	0.42	**J53**	0.61	0.53	0.42
J54	0.61	0.53	0.42	**J54**	0.61	0.53	0.42
J55	0.61	0.53	0.42	**J55**	0.61	0.53	0.42
J56	0.61	0.53	0.42	**J56**	0.61	0.53	0.42
J57	0.62	0.53	0.42	**J57**	0.62	0.53	0.42
J58	0.63	0.53	0.43	**J58**	0.63	0.53	0.43
J59	0.72	0.55	0.45	**J59**	0.71	0.55	0.45
J60	0.94	0.82	0.63	**J60**	0.95	0.82	0.63
J61	1.44	1.23	0.84	**J61**	1.39	1.20	0.82
J62	1.5	1.5	1.40	**J62**	1.5	1.5	1.38
J63	1.5	1.5	1.44	**J63**	1.5	1.5	1.42
J64	1.5	1.5	1.5	**J64**	1.5	1.5	1.5
J65	1.5	1.5	1.5	**J65**	1.5	1.5	1.5
J66	1.5	1.5	1.5	**J66**	1.49	1.5	1.5
J67	1.5	1.5	1.5	**J67**	1.5	1.5	1.5
J68	1.5	1.5	1.5	**J68**	1.5	1.5	1.5
J69	1.5	1.5	1.5	**J69**	1.5	1.5	1.5
J70	1.5	1.5	1.5	**J70**	1.5	1.5	1.5
J71	1.5	1.5	1.5	**J71**	1.49	1.5	1.5
J72	1.5	1.5	1.5	**J72**	1.5	1.5	1.5
J73	2	1.77	1.64	**J73**	1.66	1.65	1.63
J74	2	2	2	**J74**	2	2	2
J75	2	2	2	**J75**	2	2	2
J76	2	2	2	**J76**	2	2	2
J77	2	2	2	**J77**	2	2	2
J78	2	2	2	**J78**	2	2	2
J79	2	2	2	**J79**	2	2	2
J80	2	2	2	**J80**	2	2	2
J81	2	2	2	**J81**	2	2	2
J82	2	2	2	**J82**	2	2	2
J83	2	2	1.96	**J83**	2	2	1.96
J47	1.46	1.38	1.29	**J47**	0.9	0.81	0.69
J46	1.5	1.5	1.49	**J46**	0.92	0.84	0.71
J45	1.5	1.5	1.5	**J45**	0.93	0.84	0.71
J44	1.5	1.5	1.5	**J44**	0.94	0.85	0.71
J43	1.5	1.5	1.5	**J43**	0.96	0.86	0.71
J42	1.5	1.5	1.5	**J42**	0.98	0.87	0.72
J41	1.5	1.5	1.5	**J41**	1.0	0.89	0.73
J40	1.5	1.5	1.5	**J40**	1.03	0.91	0.75
				J84	1.07	0.95	0.78
				J85	1.14	1.01	0.84
				J86	1.11	0.99	0.81
				J87	1.11	0.98	0.81
				J88	1.1	0.98	0.81
				J89	1.1	0.98	0.81
				J90	1.1	0.98	0.81
				J91	1.09	0.98	0.81
				J92	1.09	0.97	0.8
				J93	1.08	0.97	0.8

				J94	1.07	0.96	0.8
				J95	1.06	0.95	0.79
				J96	1.03	0.93	0.78
				J97	1	0.9	0.76
				J98	0.95	0.86	0.73
				J99	0.86	0.78	0.66
				O1	0.74	0.68	0.59
O1	1.0	0.94	0.82	**O2**	0.73	0.66	0.55

4. CONCLUSIONS

The current study aims to set up the SWMM model for the research area, and the findings show that it is capable of accurately simulating runoff and peak runoff in urban catchments. For the 5-year, 25-year, and 100-year return periods, the IDF curve indicates maximum intensities of 78.311, 106.711, and 130.145 mm/hr, respectively, at 10-minute intervals. After analyzing these three scenarios and the model's results for more clarification, the researcher concluded that:

1. A significant portion of the nodes in all three scenarios, both before and after the addition of the box drainage network, were flooded, and the amount of flooding was very high. This suggests that this may not be the most basic way to prevent flooding in the study area.
2. The current box drainage network may not have a very good effect if heavy rains fall in a short period of time because it is unable to pass all the water accumulated there. This is because the study area is a populated area and a flood-risk area. It would have been better to have a larger section and size for the box drainage network.
3. Erbil is a city that is quickly growing, and the research area's sewage system is very ancient. The entire drainage system in the area needs to be redesigned in order to prevent flooding. Sections should also be enlarged to make it easier to access water at inlets without encountering any issues in the manholes and to drain all runoff during rainstorms.

References

AGARWAL, S. & KUMAR, S. 2020. Urban Flood Modeling using SWMM for Historical and Future Extreme Rainfall Events under Climate Change Scenario. *Indian Journal of Ecology,* 47**,** 48-53.

ALISAWI, H. A. O. 2020. A sewer overflow mitigation during festival and rainfall periods: case study of Karbala. *Applied Water Science,* 10**,** 1-9.

BOOTH, D. B. 1991. Urbanization and the natural drainage system--impacts, solutions, and prognoses.

BUTLER, D. & DAVIES, J. 2011. Urban Drainage, Chapter 7. System component and design. Taylor & Francis.

CHOW, V. T., MAIDMENT, D. R. & MAYS, L. W. 1988. *Applied hydrology,* New York; London, McGraw-Hill.

DOUGLAS, I., ALAM, K., MAGHENDA, M., MCDONNELL, Y., MCLEAN, L. & CAMPBELL, J. 2008. Unjust waters: climate change, flooding and the urban poor in Africa. *Environment and urbanization,* 20**,** 187-205.

HUONG, H. T. L. & PATHIRANA, A. 2013. Urbanization and climate change impacts on future urban flooding in Can Tho city, Vietnam. *Hydrology and Earth System Sciences,* 17**,** 379-394.

MOHAMMAD, E. I., MUSTAFA, A. S. & ADHAM, A. 2021. Simulation of Storm Sewer Network Using a Storm Water Man-agement Model (SWMM), Ramadi City as a Case Study. *Anbar Journal for Engineering Sciences,* 9**,** 83-89.

PATZ, J. A., CAMPBELL-LENDRUM, D., HOLLOWAY, T. & FOLEY, J. A. 2005. Impact of regional climate change on human health. *Nature,* 438**,** 310-317.

ROSSMAN, L. 2015. Storm water management model user’s manual, version 5.1: National Risk Management Laboratory Office of Research and Development US Environmental Protection Agency 26 Martin Luther King Drive Cincinnati. OH.

BEHBAHANI, S.M. 2009. Surface water hydrology. Second edition. Tehran Press. 488 pp.